Oncology and Translational Medicine
DOI 10.1007/s10330-017-0229-9
2017, Vol. 3, No. 4, P143–P150

ORIGINAL ARTICLE

Effect of low dose fractionated radiation on reversing cisplatin resistance in ovarian carcinoma via VEGF and mTOR*

Xingyan Ju[1], Shihai liu[2], Donghai Liang[1], Tao Jiang[1], Ronghui Yuan[1], Wei Zhao[3], Hongsheng Yu[1] (✉)

[1] Department of Oncology, the Affiliated Hospital of Qingdao University, Qingdao 266003, China
[2] Department of Central Laboratory, the Affiliated Hospital of Qingdao University, Qingdao 266003, China
[3] Department of Oncology, Chinese Medical Hospital of Huangdao District, Qingdao 266003, China

Abstract

Objective To investigate the mechanism of low-dose fractionated radiation on reversing cisplatin resistance in ovarian carcinoma via vascular endothelial growth factor (VEGF) and mammalian target of rapamycin (mTOR) *in vivo*.

Methods Human cisplatin-resistant ovarian carcinoma cells (SKOV3/DDP) were injected into nude mice to establish ovarian cancer xenografts. The mice were randomly divided into three groups: a control group, a low-dose fractionated radiation (LDRFT) group, and a conventional-dose radiation group. Each group was exposed to 0 cGy, 50 cGy, and 200 cGy radiation, respectively, for 4 weeks, up to a total of 8.0 Gy. Mice in the LDFRT group were irradiated twice daily with 6 hour intermissions on day 1 and 2 of every week for a total of 4 weeks. Conventional-dose group mice were given a single 200 cGy radiation dose on the first day each week for a total of 4 weeks. Maximum horizontal and vertical diameters of the tumors were measured every other day and used to create a tumor growth curve. After 4 weeks of irradiation, we dissected the tumor tissue and calculated the tumor inhibition rate. RT-PCR detected the expression of VEGF and mTOR, and Western blots detected the expression of corresponding proteins.

Results Both LDRFT and conventional-dose radiation inhibited the growth of tumor cells, and growth of tumors in the two radiation groups compared with growth in the control group were significantly different ($P < 0.05$). The rate of tumor inhibition in the LDFRT group (37.5603%) was lower than in the conventional-dose group (47.4446%), but there was no significant difference ($P > 0.05$). Compared with the other two groups, the mRNA expression of VEGF was significantly lower in the LDFRT group ($P < 0.05$), but there was no obvious difference between the conventional-dose and control groups. There was no obvious difference in the mRNA expression of mTOR among the three groups, but the expression of the protein p-mTOR was lower in the LDFRT group ($P < 0.05$), as confirmed by Western blotting.

Conclusion LDFRT is as effective at inhibiting the growth of tumor cells as conventional-dose radiation. In addition, LDFRT could deregulate the expression of VEGF and p-mTOR, and may therefore play a vital role in reversing cisplatin resistance in ovarian cancer.

Keywords: low-dose fractionated radiation; ovarian carcinoma; resistance; SKOV3/DDP; VEGF; mTOR

Received: 13 May 2017
Revised: 11 July 2017
Accepted: 18 July 2017

Human epithelial ovarian carcinoma (EOC) is the most fatal gynecologic malignancy and the fifth leading cause of cancer-related mortality for women around the world [1-2]. Although the standard therapy for EOC (cytoreductive surgery along with platinum-based chemotherapy) is developing in effectiveness, the 5-year survival rate is merely 30% for advanced ovarian cancer patients [3]. Chemotherapy resistance is the primary cause attributed to treatment failure, which greatly reduces the lifespans of patients and their quality of life [4]. Cisplatin

✉ Corresponding to: Hongsheng Yu. Email: qdhsyu@126.com
*Supported by a grant from the Province Natural Sciences Foundation of Shandong (No. ZR2016040034).

is currently one of the most valid and commonly used chemotherapeutic drugs for treatment of ovarian cancer. Unfortunately, the progression of cisplatin resistance restricts its thorough application in ovarian cancer patients [5]. Even though understanding through research has deepened over decades, the cisplatin resistance mechanisms have not been clearly explained.

The classic survival-promoting and anti-apoptotic signaling cascade pathway, PI3K/AKT, includes vascular endothelial growth factor (VEGF) and mammalian target of rapamycin (mTOR). It is the most frequent various pathway in human cancer and regulates the progress and characteristics of the disease: the cell survival, angiogenesis, metabolism, cell cycle, motility, genomic instability, and chemo-resistance that are crucial for cancer development [6]. Previous studies have indicated that the PI3K/AKT/mTOR signaling pathway is deregulated in multiple malignancies involving ovarian, colorectal, breast, endometrial, and other malignant tumors [7]. In addition, angiogenesis is indispensable for the growth and metastasis of tumors by developing new vasculature that provides tumor tissue with essential nutrition [8]. In EOC several VEGF family members are highly expressed and play vital roles in the progression of malignant neoplasm, but their contribution in many chemo-resistant diseases remains unclear. With this accumulated knowledge, Momeny *et al* found that VEGFR2 might be associated with resistance to cisplatin [9]. The VEGF/VEGFR signaling pathway is a promising angiogenic target due to its significant role in tumor growth and angiogenesis [10–11].

Recently, radiation therapy for EOC patients has attracted major research due to the low response rate of chemotherapy caused by primary and acquired drug-resistance. The bystander effect phenomenon occurs when cells not directly irradiated display the effects of radiation damage, including genomic instability, sister chromatid exchange, DNA double-strand breaks, and micronucleus formation [12–13]. Recent experimental and clinical data have given rise to a novel treatment combining full-dose systemic chemotherapy with low-dose fractionated radiation (LDFRT) [14]. A previous study has indicated that LDFRT might heighten tumor sensitivity to subsequent chemotherapy and improve the primary site and nodal site response rate up to 90% and 60%, respectively [15]. Furthermore, LDFRT can induce immune responses and enhance antioxidant capacity [16], and induce DNA repair response in normal tissues [17], which cooperatively provide an efficacious method of local tumor control. Thus, LDFRT may serve as a valuable treatment for cisplatin-resistant ovarian cancer patients.

In this study, nude mice in a xenograft model were given LDFRT (50 cGy delivered in four fractions) and conventional-dose radiation (200 cGy) to examine whether LDFRT could reverse cisplatin resistance, which may produce a significant breakthrough in the treatment of ovarian cancer patients.

Materials and methods

Materials and cell culture

SKOV3/DDP cells were cisplatin-resistant human ovarian cancer cells purchased from the Institute of Cancer Research, Chinese Academy of Medical Sciences (Beijing, China). SKOV3/DDP cells were cultured in RPMI-1640 medium with 1% antibiotics (100 μg/mL streptomycin and 100 U/mL penicillin) and 10% fetal bovine serum (FBS) (Gibco Co, Australia) in a humidified 5% CO_2 incubator at 37 ℃.

Ovarian carcinoma xenografts in nude mice

Female BALB/C nude mice (Shanghai SLAC Laboratory Animal Company, China) aged 4–5 weeks-old and weighing 18–22 g were grown in micro-isolator cages in germ-free (GF)/specified pathogen-free (SPF) condition. Exponential growth phase SKOV3/DDP cells of 1×10^7/mL concentration were selected for the experiment under aseptic conditions. Xenotransplantations were carried out by subcutaneously injecting 2×10^6 cells into the groin near the lower left limb of each mouse. About one week later, the tumors had grown to the size of soybeans. Thirty mice were randomly divided into three groups (control group, low-dose fractionated radiation group, and conventional-dose radiation group) of ten mice each. The xenografts were established and were cultured in continuously GF/SPF conditions.

Irradiation conditions of ovarian cancer tumor-bearing nude mice

Xenografts in the control group were not exposed to radiation. The other groups were irradiated with 6 megavolt (MV) X-ray equipment. The dose verification system measured a dosage rate of 100 cGy every minute and the minimum distance from the radiation source to skin was 100 cm. Vaseline gauze of 1.5 cm thickness was used as a tissue compensator upon tumor appearance. Mice in the LDFRT group received treatment in 50 cGy fractions twice daily for 2 days with a minimum of 6 hours intermission on days 1 and 2 of every week for a total of 4 weeks; the total dose after all fractions was 8 Gy. Mice in the conventional-dose group received a single 200 cGy fraction on the first day of each week for a total of 4 weeks. The source to skin distance, dose rates, and other conditions were the same as in the LDFRT group.

Tumor growth curve

All tumors were measured for maximum horizontal diameter (a, cm) and vertical diameter (b, cm) every 2

days from the first day of radiation treatment until the mice were sacrificed. Each mouse was measured three times and the averages were recorded. The tumor volume (TV) was calculated according to the published formula: TV (cm^3)=1/2 × a × b × b. The growth curve of the tumors was drawn according to the TV.

Tumor inhibition rate

The animals were weighed every other day when the TV was measured. The mice were sacrificed 24 h after the last radiation treatment. The percentage of tumor growth suppression was then calculated by contrasting the treated groups with the control group. Tumor inhibition rate = (Average tumor weight of control group – Average tumor weight of treated groups)/Average tumor weight of control group × 100%. The tumor tissue obtained was placed in liquid nitrogen for analysis.

RNA isolation and quantitative real-time PCR (RT-PCR)

The fresh frozen tumor tissue was used to isolate total RNA with TRIzol Reagent (Invitrogen, Life Technologies, Carlsbad, CA, USA) according to the manufacturer's instructions. cDNAs were synthesized with the TAKARA Reverse Transcription Kit (Takara Bio, Dalian, China) through Taqman Reverse Reaction. Primer and SYBR Premix Ex Taq II were added to the 20 μL final reaction volume. Control gene GAPDH was purchased from Shanghai Sangon Biotech Company (China). Quantitative real-time PCR was carried out on an Applied Biosystems 7500 System. The mRNA of VEGF and mTOR were detected. All samples were tested in triplicate. The quantity of mRNA expression was analyzed with the $2^{(-\Delta\Delta CT)}$ comparative method. All primers are shown in Table 1.

Extraction of proteins and determination of protein concentrations

Using the Radio-Immunoprecipitation Assay (RIPA, Solarbio life science, Beijing, China), phenylmethane sulfonyl fluoride (PMSF) and a phosphatase inhibitor were added to fresh tumor tissue at a ratio of 100:1:1 then incubated for 30 min on ice. Lysates were gathered after centrifugation (12000 g for 5 min at 4 ℃). The Enhanced BCA Protein Assay Kit (Beyotime Biotechnology, China) was used to determine the concentrations of proteins according to the manufacturer instructions of the Broadford Protein Assay Kit. The protein sample concentrations were calculated according to the protein standard curve and the volume of the protein used. All extracted protein was stored at –80 ℃.

Table 1 Primers of relative mRNA

Relative mRNA	Forward Sequence	Reverse Sequence
VEGF	TCCCGGTATAAGTCCTGGAG	ACAAATGCTTTCTCCGCTCT
mTOR	TGCTGAAGGACTCATCATCG	CAGTTCAGACCAGCAGGAACA
GAPDH	GTCTCCTCTGACTTCAACAGCG	ACCACCCTGTTGCTGTAGCCAA

Western blot analysis

Equivalent amounts of proteins (50 μg) for each sample were electrophoresed on 6%–10% SDS-PAGE gel. Then proteins were transferred to PVDF membranes for 1.5 h at 300 mA. Membranes containing proteins were blocked at room temperature (RT) for 2 h with 5% non-fat milk in TBS including 1% Tween-20 (T-TBS). Primary antibodies were incubated overnight at 4 ℃. Primary antibodies (mTOR, p-mTOR) were purchased from Cell Signaling Technology Company (USA). VEGF antibody was purchased from Abcam (England). GAPDH was purchased from Beijing Comwin Biotech Co, Ltd (China). Membranes were washed four times for 10 min each time, and incubated with the approximate horseradish peroxidase-marked anti-rabbit for 1 h at RT. Membranes were washed in the same way. Secondary antibody was purchased from Abcam (England). Signals were detected by applying a SuperEnhanced Chemiluminescence Detection Kit with the Bio-Rad GelDoc XR Gel Documentation System. Pixel densitometry was quantified by the ImageJ® software. Each experiment was performed in triplicate. Visual signals were shown in Fig. 1.

Statistical analysis

The experimental data were calculated using SPSS Version 19.0 and performed as mean ± S.E. Control

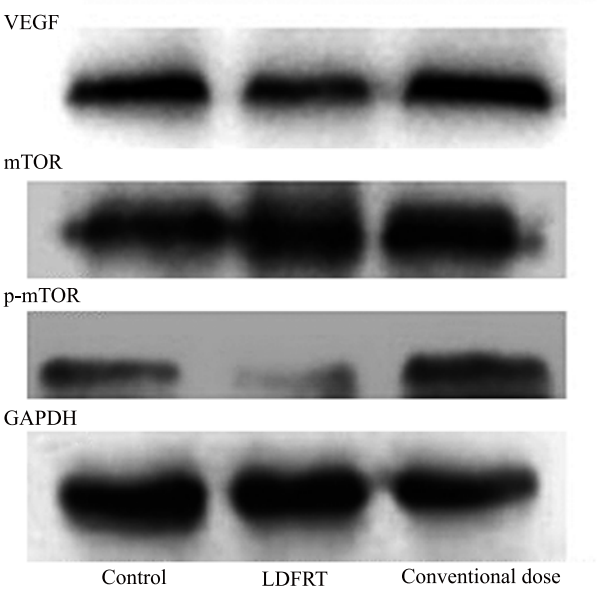

Fig. 1 Protein in three groups were assessed by Western blot

and treated group comparisons were made by one-way ANOVA followed by the LSD *t*-test. Results were defined as statistically significant at $P < 0.05$. Tumor inhibition rates were contrasted with a two-tailed independent sample *t*-test.

Results

Xenotransplantations of ovarian cancer

When SKOV3/DDP cells were in the logarithmic growth phase and the viability of the cells was greater than 95%, 2×10^6 cells were implanted into each nude mouse. Tumor formation rate was 92.31% 7 days after implantation and soybean-sized tumor nodules could be seen. After 4 weeks of irradiation, 3, 2, and 3 mice had died in the control group, LDFRT group, and conventional-dose group, respectively. Survival rates (as shown in Fig. 2) in the three groups were not significantly different ($P > 0.05$). Xenotransplantation pictures appear in Fig. 3.

Tumor growth curve

From the first day after irradiation, the size of the tumor tissue was measured every other day until the last radiation fraction was administered, and the data are shown in Table 2 and Fig. 4. The tumor volumes in the LDFRT and conventional-dose groups were lower than in the control group ($P < 0.05$). Tumor sizes in the LDFRT group and conventional-dose group had no significant difference ($P > 0.05$).

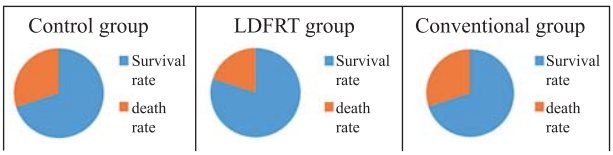

Fig. 2 Survival rates in the three groups. LDFRT group: Low-dose fractionated radiation group. There was no significant difference ($P > 0.05$) in survival rate among the three groups

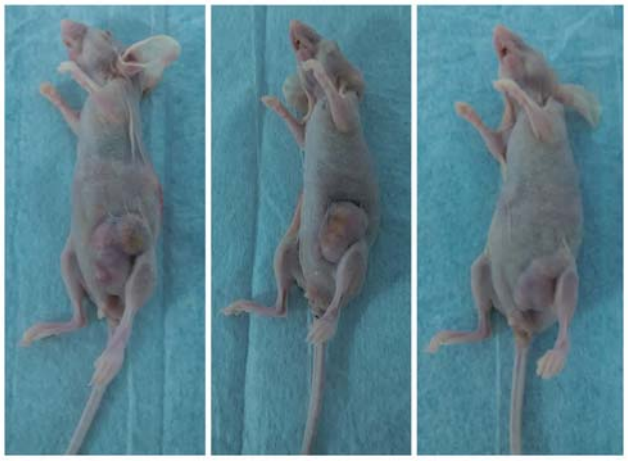

Fig. 3 Xenotransplantation pictures

Inhibition effects on tumor growth

All nude mice in the three groups were sacrificed 24 h after the last radiation treatment. All tumor nodules were dissected and the tumor tissue was weighed using a balance with 0.01 g accuracy. The weight of the tumor tissues in the LDFRT group and the conventional-dose group were much lower than in the control group ($P < 0.05$). There was no significant difference in tumor weight between the LDFRT and conventional-dose groups ($P > 0.05$). Tumor weights are shown in Table 3, Fig. 5 and Fig. 6.

The results of mRNA expression level of VEGF

After RT-PCR and delineation of the kinetic curves accompanying PCR amplification, the mRNA expression level of VEGF was calculated. As shown in Table 4 and Fig. 7, all mice in the LDFRT group showed lower mRNA expression of VEGF ($P < 0.05$) than the mice in the

Table 2 Effects of low-dose radiation on tumor growth (cm^3)

Days after radiation	Control group	LDFRT group**	Conventional-dose group*
1	0.061±0.042	0.097±0.050	0.068±0.038
3	0.159±0.095	0.225±0.117	0.186±0.109
5	0.397±0.191	0.422±0.203	0.393±0.212
7	0.502±0.207	0.443±0.228	0.424±0.243
9	0.769±0.235	0.485±0.213	0.573±0.281
11	0.862±0.297	0.442±0.157	0.571±0.216
13	1.117±0.425	0.561±0.209	0.719±0.248
15	1.220±0.474	0.525±0.165	0.620±0.253
17	1.221±0.376	0.526±0.157	0.683±0.278
19	1.320±0.400	0.571±0.227	0.617±0.302
21	1.438±0.478	0.569±0.246	0.592±0.289

LDFRT group: Low-dose fractionated radiation group; LDFRT and conventional groups compared with control group, * $P < 0.05$; LDFRT group compared with conventional group, ** $P > 0.05$.

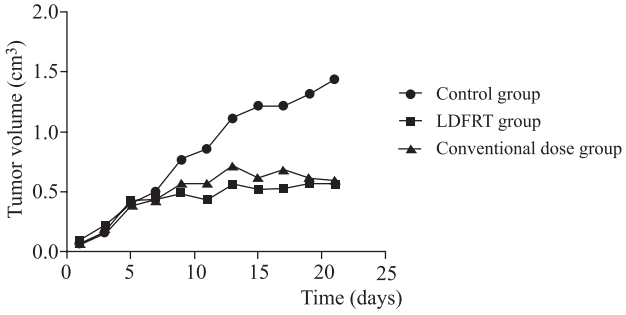

Fig. 4 The curve of tumor growth. In the first 5 days there was no obvious difference in tumor sizes among three groups. After 5 days, tumor tissues in the control group were growing faster than in the other two groups and had the largest tumor volume

Table 3 Tumor weight of each group

Group	Tumor weight (g)
Control group	1.481 ± 0.586
LDFRT group	0.925 ± 0.319**
Conventional-dose group	0.778 ± 0.334*

LDFRT group: low-dose fractionated radiation group. Compared with control group, * $P < 0.05$; Compared with conventional group, ** $P > 0.05$

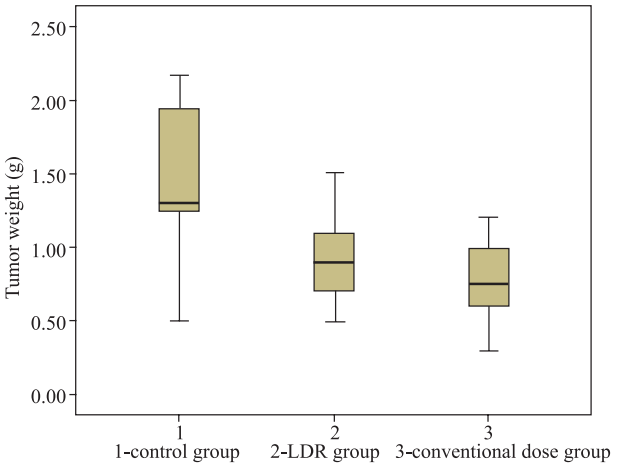

Fig. 5 Tumor weight of each group. Group 2 and 3 compared with 1, * $P < 0.05$; group 2 compared with 3, ** $P > 0.05$

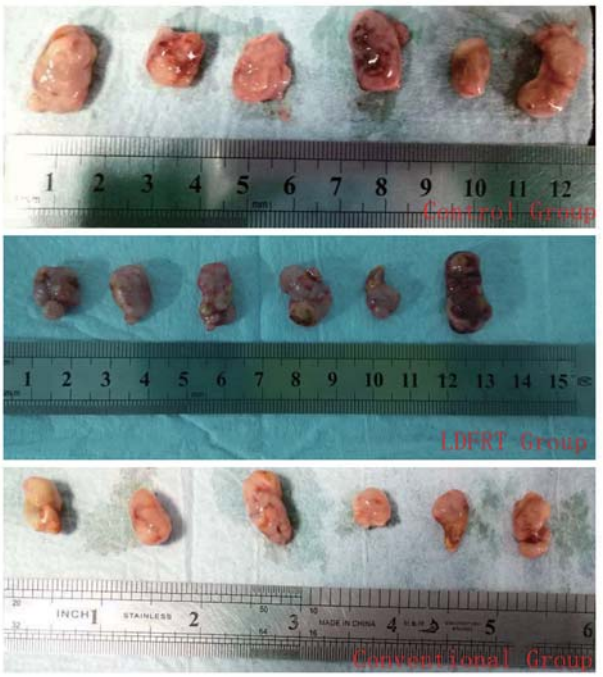

Fig. 6 Tumors of each group

control and conventional-dose groups, but there was no significant difference between expression in the control group and conventional-dose group ($P > 0.05$). Primers of VEGF, mTOR, and GAPDH were shown as listed in Table 1.

Table 4 Real-Time PCR for detecting mRNA expression of VEGF

Groups	Δ Δ CT	$2^{-\Delta\Delta CT}$
control group	3.313±0.264	1±0
LDFRT group	9.083±1.459	0.025±0.018*
conventional dose group	3.165±0.749	1.299±0.793**

LDFRT group: low-dose fractionated radiation group. $\Delta CT = CT_{target\ gene} - CT_{GAPDH}$, $\Delta\Delta CT = \Delta CT_{treat\ group} - \Delta CT_{control\ group}$. VEGF expression in the LDFRT group was significantly decreased (* $P < 0.05$) compared with the control and conventional-dose groups (** $P > 0.05$ compared with control group)

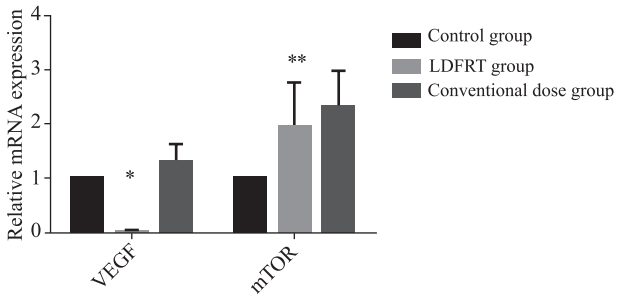

Fig. 7 Relative mRNA expression. VEGF was significantly decreased (* $P < 0.05$) compared with the other two groups; There was no significant difference in mTOR among the three groups (** $P > 0.05$)

Table 5 Real-Time PCR for detecting mRNA expression of mTOR

Groups	Δ Δ CT	$2^{-\Delta\Delta CT}$
control group	5.155±1.937	1±0
LDFRT group	5.084±1.561	1.961±1.096*
conventional dose group	4.341±1.036	2.312±1.631

LDFRT group: low-dose fractionated radiation group. $\Delta CT = CT_{target\ gene} - CT_{GAPDH}$, $\Delta\Delta CT = \Delta CT_{treat\ group} - \Delta C_{control\ group}$. No obvious difference among the three groups (* $P > 0.05$) for the mRNA expression of mTOR.

The results of mRNA expression level of mTOR

After RT-PCR and delineation of the kinetic curves accompanying PCR amplification, the mRNA expression levels of mTOR were calculated. As shown in Table 5 and Fig. 7, there was no obvious difference in the expression level of mTOR among the three groups ($P > 0.05$).

The analysis of related protein expression by Western blotting

In this analysis, GAPDH was chosen as an internal control. As Fig. 1 and Fig. 8 display, the protein expression of VEGF and p-mTOR were significantly decreased ($P < 0.05$) in the LDFRT group when compared with the control and conventional-dose groups. In addition, as the figure shows, there was no obvious difference in the protein expression of mTOR in the three groups ($P >$

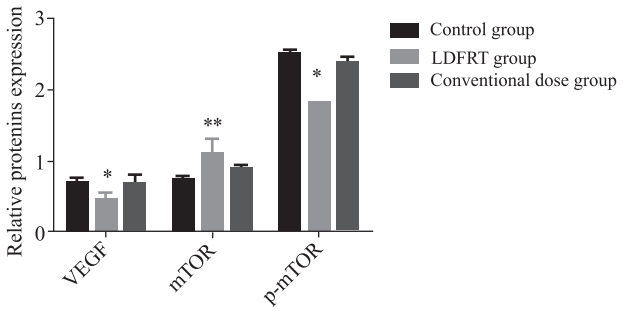

Fig. 8 Relative protein expression. Proteins of VEGF and p-mTOR in the LDFRT group were significantly decreased compared with other groups,* $P < 0.05$; There was no obvious difference in the protein expression of mTOR in the three groups, ** $P > 0.05$

0.05).

Discussion

Epithelial ovarian cancer is a leading cause of gynecological cancer-related death [18]. In China, there will be about 52,100 patients newly diagnosed with EOC, as predicted in 2015, and over 61 deaths due to EOC on average per day [19]. Although treatment via debulking surgery combined with platinum-based chemotherapy is improving, a diagnosis of advanced stage and intrinsic or acquired resistance to chemotherapy drugs (cisplatin) results in high mortality [20]. Thus, identifying the mechanism of EOC cisplatin resistance and an effective approach to reversing it are of crucial importance.

The contribution of radiotherapy to the treatment of EOC cannot be ignored. Low-dose fractionated radiation therapy (LDFRT) has been proposed as a chemo-sensitizer because of the palpable side effects of conventional-dose (whole-abdomen dose of 2250 to 3000 cGy, pelvic dose of 4500 to 5000 cGy) radiation. A series of observational studies have shown that human epithelial ovarian cancer cells and oocyte cells are especially sensitive to radiation, with a dose of 200 cGy to 600 cGy needed to sterilize cells [21–22]. In addition, faith in the potential of LDFRT (<100 cGy) is increasing due to the report by Joiner *et al* that there is an initial phase of hyper-radiosensitivity (HRS) with doses ranging from 1 to 80 cGy [23]. The HRS caused by LDFRT is an unparalleled radiobiological phenomenon, which suggests that unlike high-dose radiation, HRS does not stimulate cellular repair mechanisms, which explains the presence of HRS without radiation resistance as measured *in vitro* [24].

As a member of the PI3K/AKT signaling pathway, vascular endothelial growth factor (VEGF) is overexpressed in EOC, and contributed to chemo-resistance. Studies suggested that high expression of VEGF ligands and their corresponding receptors could accelerate malignant progression and have a negative effect on prognosis in EOC [25, 26]. The hypoxic nature of the tumor microenvironment could increase the expression of VEGF, reducing the efficiency of radiotherapy and chemotherapy [27]. Actually, our previous studies suggested that low-dose radiation could reduce VEGF expression by mobilizing the immune system [28]. Therefore, we hypothesize that LDFRT may be a meaningful approach to reversing chemotherapy resistance by regulating the mRNA expression of VEGF. As expected, our results as shown in Table 4 and Fig. 7 indicated that the expression of VEGF was decreased in the LDFRT group compared with the control and conventional-dose groups. One of the most important reasons is that for solid tumors larger than 1-2mm, new vessels are formed in the tumor to providing nutrition, which is called the "balance of angiogenesis switch" [29]. Furthermore, the inhibition of VEGF obstructs the PI3K/AKT signaling pathway during the S period and induces G2 arrest and apoptosis, which plays a vital role in enhancing SKOV3/DDP sensitivity to chemotherapy [30]. Besides, our results are consistent with the study of Santulli *et al*, which showed that synthesized VEGF-mimicking peptides binding to their receptors activate the VEGF-induced signaling pathway and induce angiogenesis [31]. Thus, we may reach the conclusion that LDFRT could inhibit the expression of VEGF, enhancing the sensitivity of SKOV3/DDP to cisplatin.

PI3K/AKT/mTOR signaling pathway activation could cause an increase in chemotherapy resistance, invasion, migration, and cell proliferation in many malignancies. For instance, the abnormal activation of the PI3K/AKT/mTOR signaling pathway is associated with gefitinib-resistance and a terrible prognosis in NSCLC patients [32]. Equivalently, in EOC patients, an altered or mutated PI3K/AKT/mTOR signaling pathway could result in chemotherapy resistance as well as tumorigenesis and the progression of the disease [33]. Moreover, using authoritative anticancer drugs to suppress the activation of the PI3K/AKT/mTOR signaling pathway has shown promise in a series of experimental studies [34]. Thus, we assumed that LDFRT could reverse chemo-resistance by regulating the activation of the PI3K/AKT/mTOR signaling pathway based on the effects of anti-angiogenesis.

As shown in Table 5, Fig. 1 and Fig. 7, our results suggest that there was no obvious difference in the expression of mTOR mRNA or related proteins in the three groups. However, the expression of the activated form of mTOR, phosphorylated mTOR (p-mTOR), was significantly decreased in the LDFRT group compared with the other two groups, which is consistent with several previous studies that considered p-mTOR to be related to drug resistance. Mabuchi *et al* declared that the expression of p-mTOR in cisplatin-resistant EOC cells is higher than in cisplatin-sensitive cells, and that cells with

overexpressed p-mTOR have greater susceptibility to the inhibitor of mTOR (RAD001) [35]. The studies may provide a plausible explanation as to why higher p-mTOR levels contribute to cisplatin resistance in EOC. In addition, PI3K/AKT/mTOR signaling pathway activation could restrain cisplatin-initiated apoptosis of EOC, resulting in cisplatin resistance [36]. Furthermore, our previous studies has already confirmed that regulating the PI3K/AKT signaling pathway with low-dose radiation could reverse cisplatin resistance. Thus, our study may support the conclusion that LDFRT could reverse cisplatin resistance in ovarian cancer cells by deregulating the expression of p-mTOR *in vivo*.

In this study, we explored a potential mechanism for reversing the resistance of SKOV3/DDP to cisplatin chemotherapy through treating nude mice xenografts with different doses of radiation. The results suggest that LDFRT could significantly reverse resistance and enhance the sensitivity of SKOV3/DDP to cisplatin by decreasing the expression of VEGF and p-mTOR, in turn inhibiting the signaling pathway of PI3K/AKT/mTOR activation.

Acknowledgements

We thank Prof. Shihai Liu for offering technical assistance and insightful suggestions during the whole experiment process.

Conflicts of interest

The authors declare that they have no competing conflicts of interests.

References

1. Haley J, Tomar S, Pulliam N, *et al*. Functional characterization of a panel of high-grade serous ovarian cancer cell lines as representative experimental models of the disease. Oncotarget, 2016, 7: 32810–32820.
2. Ferlay J, Soerjomataram I, Dikshit R, *et al*. Cancer incidence and mortality worldwide: sources, methods and major patterns in GLOBOCAN 2012. Int J Cancer, 2015, 136: E359–386.
3. Jemal A, Siegel R, Xu J, *et al*. Cancer statistics, 2010. CA Cancer J Clin, 2010, 60: 277–300.
4. Nguyen HG, Ravid K. Tetraploidy/aneuploidy and stem cells in cancer promotion: The role of chromosome passenger proteins. J Cell Physiol, 2006, 208: 12–22.
5. Armstrong DK. Relapsed ovarian cancer: challenges and management strategies for a chronic disease. Oncologist, 2002, 7 Suppl 5: 20–28.
6. Fruman DA, Rommel C. PI3K and cancer: lessons, challenges and opportunities. Nat Rev Drug Discov, 2014, 13: 140–156.
7. Bartholomeusz C, Gonzalez-Angulo AM. Targeting the PI3K signaling pathway in cancer therapy. Expert Opin Ther Targets, 2012, 16: 121–130.
8. Hicklin DJ, Ellis LM. Role of the vascular endothelial growth factor pathway in tumor growth and angiogenesis. J Clin Oncol, 2005, 23: 1011–1127.
9. Momeny M, Sabourinejad Z, Zarrinrad G, *et al*. Anti-tumour activity of tivozanib, a pan-inhibitor of VEGF receptors, in therapy-resistant ovarian carcinoma cells. Sci Rep, 2017, 7: 45954.
10. Spannuth WA, Sood AK, Coleman RL. Angiogenesis as a strategic target for ovarian cancer therapy. Nat Clin Pract Oncol, 2008, 5: 194–204.
11. Vecchione A, Belletti B, Lovat F, *et al*. A microRNA signature defines chemoresistance in ovarian cancer through modulation of angiogenesis. Proc Natl Acad Sci U S A, 2013, 110: 9845–9850.
12. Mothersill C, Seymour RJ, Seymour CB. Bystander effects in repair-deficient cell lines. Radiat Res, 2004, 161: 256–263.
13. Postiglione I, Chiaviello A, Palumbo G. Twilight effects of low doses of ionizing radiation on cellular systems: a bird's eye view on current concepts and research. Med Oncol, 2010, 27: 495–509.
14. Nguyen DM, Parekh PR, Chang ET, *et al*. Contribution of Dual Oxidase 2 (DUOX2) to hyper-radiosensitivity in human gastric cancer cells. Radiat Res, 2015, 184: 151–160.
15. Mothersill C, Seymour CB. Radiation-induced bystander effects – implications for cancer. Nat Rev Cancer, 2004, 4: 158–164.
16. Farooque A, Mathur R, Verma A, *et al*. Low-dose radiation therapy of cancer: role of immune enhancement. Expert Rev Anticancer Ther, 2011, 11: 791–802.
17. Liu SZ, Cai L, Sun JB. Effect of low-dose radiation on repair of DNA and chromosome damage. Acta Biol Hung, 1990, 41: 149–157.
18. Wang Y, Jin X, Song H, *et al*. AEG-1 as a predictor of sensitivity to neoadjuvant chemotherapy in advanced epithelial ovarian cancer. Onco Targets Ther, 2016, 9: 2385–2392.
19. Chen W, Zheng R, Baade PD, *et al*. Cancer statistics in China, 2015. CA Cancer J Clin, 2016, 66: 115–132.
20. Jemal A, Siegel R, Ward E, *et al*. Cancer statistics, 2009. CA Cancer J Clin, 2009, 59: 225–249.
21. Adriaens I, Smitz J, Jacquet P. The current knowledge on radiosensitivity of ovarian follicle development stages. Hum Reprod Update, 2009, 15: 359–377.
22. Wallace WH, Thomson AB, Kelsey TW. The radiosensitivity of the human oocyte. Hum Reprod, 2003, 18: 117–121.
23. Joiner MC. Induced radioresistance: an overview and historical perspective. Int J Radiat Biol, 1994, 65: 79–84.
24. Marples B, Greco O, Joiner MC, *et al.* Molecular approaches to chemo-radiotherapy. Eur J Cancer, 2002, 38: 231–239.
25. Decio A, Taraboletti G, Patton V, *et al*. Vascular endothelial growth factor c promotes ovarian carcinoma progression through paracrine and autocrine mechanisms. Am J Pathol, 2014, 184: 1050–1061.
26. Boocock CA, Charnock-Jones DS, Sharkey AM, *et al*. Expression of vascular endothelial growth factor and its receptors flt and KDR in ovarian carcinoma. J Natl Cancer Inst, 1995, 87: 506–516.
27. Huang G, Chen L. Tumor vasculature and microenvironment normalization: a possible mechanism of antiangiogenesis therapy. Cancer Biother Radiopharm, 2008, 23: 661–667.
28. Yu HS, Liu ZM, Yu XY, *et al*. Low-dose radiation induces antitumor effects and erythrocyte system hormesis. Asian Pac J Cancer Prev, 2013, 14: 4121–4126.
29. Elbarghati L, Murdoch C, Lewis CE. Effects of hypoxia on transcription factor expression in human monocytes and macrophages. Immunobiology, 2008, 213: 899–908.
30. Kurosu T, Nagao T, Wu N, *et al*. Inhibition of the PI3K/Akt/GSK3 pathway downstream of BCR/ABL, Jak2-V617F, or FLT3-ITD downregulates DNA damage-induced Chk1 activation as well as G2/M arrest and prominently enhances induction of apoptosis. PLoS

One, 2013, 8: e79478.
31. Santulli G, Ciccarelli M, Palumbo G, *et al*. *In vivo* properties of the proangiogenic peptide QK. J Transl Med, 2009, 7: 41.
32. Janmaat ML, Kruyt FA, Rodriguez JA, *et al*. Response to epidermal growth factor receptor inhibitors in non-small cell lung cancer cells: limited antiproliferative effects and absence of apoptosis associated with persistent activity of extracellular signal-regulated kinase or Akt kinase pathways. Clin Cancer Res, 2003, 9: 2316–2326.
33. Dobbin ZC, Landen CN. The importance of the PI3K/AKT/MTOR pathway in the progression of ovarian cancer. Int J Mol Sci, 2013, 14: 8213–8227.
34. Mabuchi S, Altomare DA, Cheung M, *et al*. RAD001 inhibits human ovarian cancer cell proliferation, enhances cisplatin-induced apoptosis, and prolongs survival in an ovarian cancer model. Clin Cancer Res, 2007, 13: 4261–4270.
35. Mabuchi S, Kawase C, Altomare DA, *et al*. mTOR is a promising therapeutic target both in cisplatin-sensitive and cisplatin-resistant clear cell carcinoma of the ovary. Clin Cancer Res, 2009, 15: 5404–5413.
36. Peng DJ, Wang J, Zhou JY, *et al*. Role of the Akt/mTOR survival pathway in cisplatin resistance in ovarian cancer cells. Biochem Biophys Res Commun, 2010, 394: 600–605.

DOI 10.1007/s10330-017-0229-9
Cite this article as: Ju XY, Liu SH, Liang DH, *et al*. Effect of low dose fractionated radiation on reversing cisplatin resistance in ovarian carcinoma via VEGF and mTOR. Oncol Transl Med, 2017, 3: 143–150.